Development of an Automated and Artificial Intelligence Assisted Pressure Chamber for Stem Water Potential Determination

Caio Mucchiani^a, Konstantinos Karydis^a

^aUniversity of California Riverside, Riverside, United States

ARTICLE INFO

Keywords: agricultural automation agricultural robotics artificial intelligence assisted visual perception stem water potential water stress

ABSTRACT

The pressure chamber (or Scholander chamber) is widely adopted for determining stem water potential (which is linked to plant water status) due to its simplicity, relative portability, and capacity to enable direct measurements. The method also serves as a reference when validating and calibrating other techniques. Despite its significant utility, the current form of the pressure chamber method is very labor-intensive, resulting in infrequent and spatially sparse sampling. Furthermore, the typical use of a compressed gas (usually nitrogen) cylinder to build up the pressure inside the chamber can cause safety issues (e.g., projectiles caused by pressure) and practical concerns (e.g., gas cylinder changes that may increase measurement time). In addition, the determination of the instance xylem water appears can vary depending on the experience of the user. For these reasons, automation and artificial intelligence (AI) technologies can be integrated to improve the current standard of practice in determining stem water potential. This work presents the development and testing of an automated pressure chamber that leverages machine vision to help determine the status of xylem wetness, a critical step toward full autonomy in stem water potential determination. The work contributes both to pneumatic actuation, whereby an air compressor and on-board electronics are employed to make the chamber fully controllable via software, and to visual perception, whereby a miniature camera and on-board electronics are integrated to provide easily visible, accessible, and real-time video feed on the excised end of a leaf's stem. Further, an AI-based object detection algorithm is deployed to determine the xylem's wetness status automatically. Several experiments with in-situ data collection demonstrate the efficiency of our system under both (semi-)manual and automatic (AI-assisted) modes of operation, thus confirming that our method can help enhance the current standard-of-practice pressure chamber method to determine stem water potential in a faster, more affordable, accurate, and repeatable manner.

1. Introduction

- The pressure chamber (also known as the Scholander chamber) is a well-known procedure to help assess stem
- water potential (Scholander et al., 1964). Stem water potential (SWP) is an important metric to approximate plant
- 4 water stress (McCutchan and Shackel, 1992), which in turn is critical for improving water utilization and crop yield
- quantity and quality (and grower profits) (Fulton et al., 2014; Schaible and Aillery, 2012; Vellidis et al., 2016) across
- 6 different types of plants but especially specialty crops and orchards (Rossello et al., 2019). The method involves the
- partial sealing of a cut leaf inside the pressure chamber with the excised end of the stem outside of the chamber. The
- 8 pressure inside the chamber increases until the point of zylem water expulsion from the excised leaf's end. At this
- 9 point, the applied pressure can be selected as the balancing pressure. Although weather and sunlight variability may

^{*}We gratefully acknowledge the support of USDA-NIFA # 2021-67022-33453, NSF # CMMI-2326309, and the University of California under grant UC-MRPI M21PR3417. Any opinions, findings, and conclusions or recommendations expressed in this material are those of the authors and do not necessarily reflect the views of the funding agencies.

^{*(}Principal) Corresponding author: K. Karydis

aciocesr@ucr.edu (C. Mucchiani); kkarydis@ece.ucr.edu (K. Karydis)
ORCID(s): 0000-0001-5471-9270 (C. Mucchiani); 0000-0002-1144-8260 (K. Karydis)

still affect single measurement reliability (Schaible and Aillery, 2012), the pressure chamber method is still largely employed despite the introduction of proximal and remote alternatives (e.g., Dhillon et al. (2017); Gonzalez-Dugo 11 et al. (2013)) since it does not require rigorous temperature control or delicate instrumentation. It also serves as the 12 calibration reference or baseline for other methods (Oosterhuis and Wullschleger, 1989; Awad-Allah, 2020), namely 13 sample-destructive methods of determining water status including the isopiestic psychrometer (Boyer and Knipling, 14 1965), the osmometer (Ball and Oosterhuis, 2005) relying on the linear relationship between plant water to solute in 15 determining osmotic potential, and the pressure probe (Husken et al., 1978) which determines the turgor pressure of 16 a plant. These emphasize the method's importance to the community. A detailed comparison of the pressure chamber 17 method against other sample-destructive methods to determine plant water status is provided in Mucchiani et al. (2024). 18 That work also discusses the potential of integrating automation and artificial intelligence (AI) across such methods 19 and argues about the significant potential afforded by the pressure chamber. 20

However, there currently exist some limitations in the pressure chamber method (Levin, 2019; Donovan et al., 2001; Rodriguez-Dominguez et al., 2022). Its primary limitation is that it is a very labor-intensive process (Goldhamer et al., 2001). Leaves have to be taken from multiple trees across a field, and, depending on plant stress, it might take a relatively long time to complete each measurement (Elsayed et al., 2011). In turn, this affects scalability to larger fields and can hinder spatio-temporally dense sampling which is essential to accurately map the plant stress condition across a field. In addition, some aspects of the pressure chamber method can be particularly error-prone, thus introducing measurement variability and imprecision. Typically, a user has to load a leaf at its stem to the chamber via a gasket seal. If the seal is tightened too much, it will clog the xylem water flow. A user must also look through a magnifying glass toward the stem's excised end to determine xylem water expression. Even under ideal visual conditions of the environment and user's eyesight, users of different experience levels will typically provide a different SWP assessment. Further, because of the high-pressure buildup in certain cases, the method can be dangerous if not conducted carefully (for instance not securing the gasket seal properly).

There currently exist two main chamber form factors that are sold commercially and are employed in practice: a manual "pump-up" and a semi-automatic "suit-case-like" chamber.² The former essentially works like a hand pump, whereby repeated upward/downward strokes increase the pressure inside the chamber. As the pressure inside the chamber builds up, it becomes harder and physically strenuous to keep increasing the pressure. There is also too much relative motion involved, which, as we discuss later, is undesirable in the context of our work. The manual chamber has a lower cost of acquisition and operation. It is easily portable, and hence a user can walk around the field and directly make measurements on the spot. The latter "suit-case-like" chamber is a static device where pressurization

21

23

31

32

33

34

35

36

¹ To be more exact, by relatively long time here we mean about 5 minutes. While on an absolute value scale this amount of time may appear reasonable, typically many leaves need to be sampled and undergo the SWP process.

² For information on these models we refer the reader to the PMS Instrument Company website at https://www.pmsinstrument.com/.

happens through an external compressed gas cylinder. The user sets the flow rate of gas into the chamber and then looks through the magnifying glass with no other physical motion involved. Oftentimes, these form-factor chambers come with a digital pressure gauge, which helps evaluate SWP. Compared to the manual pressure buildup case, this 42 chamber removes some of the variability associated with relative motion and is less physically strenuous. However, 43 it has a considerably higher cost to acquire and maintain (compressed gas consumption can be very fast, especially for less-experienced users). It is also much heavier, hence it needs to be loaded onto some form of tractor or cart 45 which needs to be driven around the field. Interestingly, despite these limitations, the pressure chambers have remained 46 mostly the same since their early years of introduction. From a research perspective, the work of Villagrán et al. (2011) 47 introduced a control system to increase and terminate pressure, but it was only tested in simulation; neither a physical prototype nor a comparison of attained results against the conventional approach were provided. Except for only a few 49 modifications such as integrating digital pressure gauges and improved mechanical construction, no other automation 50 and AI aspects have been implemented in physical commercial chambers to date (Mucchiani et al., 2024). 51

In this work, we developed and tested an automated and AI-assisted system for the SWP pressure chamber method. Our work aims to improve SWP measurement in accuracy, consistency, safety, affordability, and accessibility, contributing to both pneumatic actuation and visual perception to help enable automation and AI integration into the chamber itself. Specifically, our developed system includes a single-board computer, a microcontroller, relays and solenoid valves, an air compressor, and a miniature camera with a specialized lens. The camera points directly toward the excised end of the stem when the leaf is mounted into the chamber. The combined system was designed to attach directly on top of a commercially available pressure chamber (specifically of the static semi-automatic form), and it can live stream the camera feed either to the immediate user via a connected monitor or to any remote user via HTTP. Our system allows for two different modes of operation, manual and automatic. The manual mode requires user input throughout all measurement steps, i.e. pressurization, detection of water in the xylem, halt of the pressure, and depressurization. In contrast, the automatic mode can pressurize, perform AI-assisted detection of xylem water, and halt autonomously. Both operation modes of the system were tested in in-situ SWP analysis of avocado tree leaves to determine water status, under different weather conditions.

It is worth highlighting that there are several steps toward fully automating the SWP determination process, as outlined in Fig. 1. In previous related efforts, we have focused on joint task and motion planning algorithm development to determine how to sample in an energy-efficient manner (Kan et al., 2021); hardware development of a custom leaf cutting end-effector and associated actuation-perception integration for autonomous leaf cutting (Campbell et al., 2022); full 3D field reconstruction for localization under the canopy (Teng et al., 2023); as well as full in-field navigation and testing to cut and retrieve leaves (Dechemi et al., 2023). This present work focuses on the very last step where an

52

53

61

62

63

64

65

66

67

68

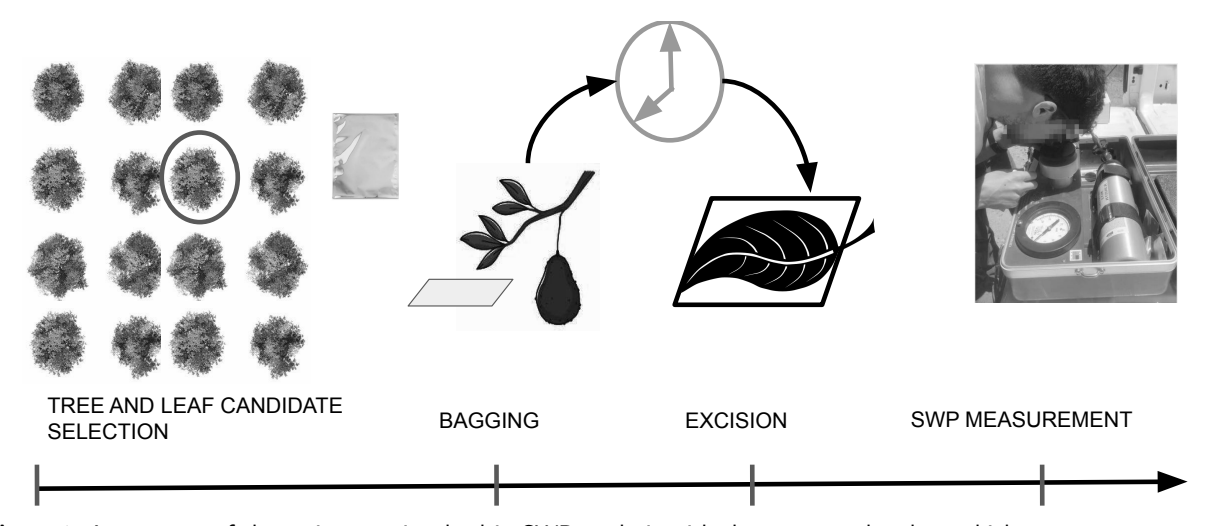


Figure 1: A summary of the main steps involved in SWP analysis with the pressure chamber, which can serve as targets for automation. This work focuses on the last step of SWP measurement.

- excised leaf is already brought to an analysis station and mounted into the chamber. Then, the process to determine its
- SWP is enhanced via our developed automated and AI-assisted pressure chamber system.

2. Materials and Methods

Our overall system's hardware components are depicted in Fig. 2. In manual mode, the human operator controls the chamber airflow (provided by the air compressor and directed by the solenoid valve) via joystick input. Since video is streamed over a network, the operator does not necessarily need to be in the vicinity of the chamber and therefore can operate the cycle remotely (apart from loading and unloading the sample). Similarly, in the automatic mode, the user has the option to control the chamber airflow (for safety); however, no input from the human operator is required between the pressurization state, data reading and recording, and exhausted state. A detailed description of the design and implementation of both modes follows.

2.1. Hardware Design

Our system contains two main components, the pneumatic actuation module and the visual perception module. The
perception module (Fig. 2, A) is placed on top of a pressure chamber (I) lid (which exposes the xylem for observation)
and consists of a custom-made 3D printed mount in PLA plastic and a Hi-Quality Pi-camera with a PT3611614M10MP
form C-mount lens. The specific lens was added to achieve the best focus and resolution on the xylem, as shown in
Fig. 2 (right). Live camera feed can be streamed via an HDMI connection to any type of external monitor such as a
laptop screen (L) or wirelessly via HTTP to any remote client. To offload heavy computation requirements of the object
detection method (K) from the onboard (host) computer while also allowing real-time data processing, a GPU-enabled
laptop (L) was also used.

Regarding the actuation module, there are two subcomponents: control and computing electronics, and pneumatics. For the former, we utilized a Raspberry Pi (E) as a host on-board computer and an Arduino (F) for the implementation 91 of both manual and autonomous modes of operation. We selected those components due to their demonstrated 92 utility across applications and their sufficient computational capacity to process the collected video stream from the 93 camera. Yet, other similarly rated single-board computers and microprocessors can be utilized instead. To pressurize the chamber, air input is provided by a 300 bar maximum pressure air compressor (C), which not only makes the measurement process self-contained (i.e. it removes the need to rely on the refill of gas cylinders, which is a limiting 96 factor for the number of samples measured in the field and can get costly over time) but also makes the process safer (as 97 opposed to the handling of high-pressure gas cylinders). The airflow is controlled, on a hardware level, by a three-way solenoid valve (B) which, together with the air compressor, are both connected via relays (G). A pressure sensor (D) qq is connected in line with the flow toward the pressure chamber. All components are rated to withstand at minimum the 100 pressure of 20 bar deemed sufficient for the application proposed herein. The pressure sensor was calibrated according 101 to pressure readings from the embedded gauge on the pressure chamber basis (I); calibration revealed an approximately 102 linear relation (Fig. 3). Pressure sensor data were streamed at a rate of 100 Hz. The entire system was powered by an 103 external AC/DC power supply (H). For safety purposes, SWP measurement cycles have to be initiated, and can be 104 aborted at any time, by a user via a wireless joystick (J, Logitech F710) which is connected to the on-board (host) 105 computer. 106

Considering all components listed besides the pressure chamber basis (I) and GPU computer (L), the cost for all utilized components is close to \$600 USD. In contrast, the conventional semi-automatic approach (i.e. not the manual "pump-up chamber") utilizes portable gas cylinders to build pressure inside the chamber. Based on experiments, each cylinder roughly suffices to perform 60-80 readings under 12 bar per experiment; the refilling cost is \$40 USD. Thus, our proposed system's bill of material cost can be paid off in about 15 gas cylinder refills, while at the same time it can be deployed to make continuous measurements.

2.2. Modes of Operation

107

108

109

110

111

112

113

114

115

116

117

118

119

120

The detailed operation procedure is depicted in Fig. 4. There are four operational states (organized in terms of state machine in software) each of which is mapped to a separate joystick button. Transitions among operational states are currently set to happen with the press of the appropriate button at the joystick for safety purposes; yet, they can be made fully automatic directly, by adding the appropriate guards and transition rules in the underlying state machine software. With reference to Fig. 4 the four operational states are as follows.

• State 1 (Idle): Before measurements, the air compressor remains off while the valve is positioned toward the "S1" or pressurize position.

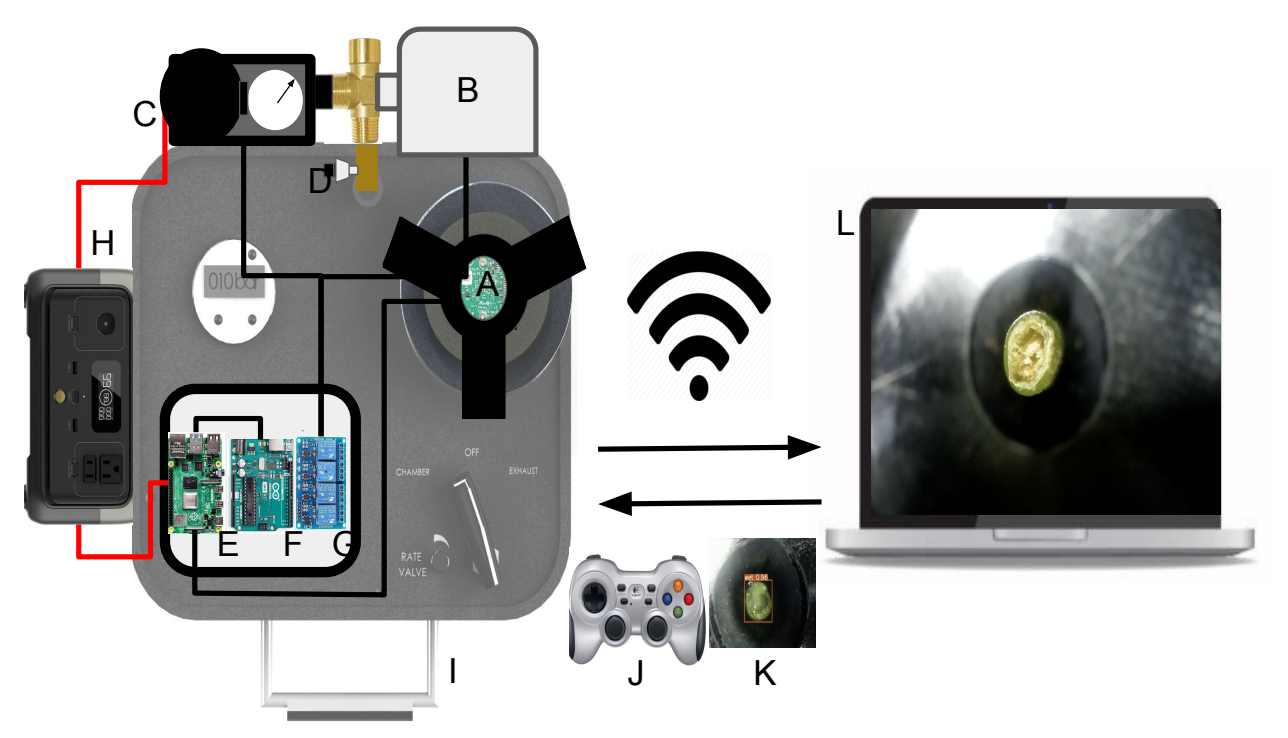


Figure 2: Hardware system implementation: (A) HQ Pi-Camera, (B) Solenoid Valve, (C)Air-Compressor, (D) Pressure sensor, (E) Raspberry Pi, (F) Arduino, (G) Relay, (H) Power Supply, (I) Pressure Chamber, (J) Joystick, (K) Object Detection Output, (L) GPU enabled computer.

- State 2 (Pressurize): When the pump is turned on by input *BT*1, air flows toward the "S1" direction, and the chamber, provided an appropriate seal, will build up pressure until the desired measurement state is achieved. This step is critical to guarantee correct measurements. To determine the transition point from dry to wet xylem, and the corresponding pressure, we proposed both manual and automatic modes. The manual mode controls the transition to the next state via joystick input *BT*2 by a human operator who observes the transition from dry to wet xylem via the real-time video feed. The automatic mode, instead, requires no input from the human operator and employs an AI-assisted visual perception algorithm (discussed below) to infer the transition from dry to wet xylem. This procedure is denoted by *DT* in our state machine.
- State 3 (Hold): Once xylem water is detected in either mode, the air compressor is turned off, while the valve is maintained in the "S1" position. This time will allow for the correct pressure to be registered and verified.
- State 4 (Release): Post measurement, the valve can be remotely switched to position S2 by BT3, and the system goes into standby mode using input BT4.

By allowing the human operator (understood here as the one in possession of the joystick) to choose between manual and automatic modes, our aim was twofold: 1) to investigate the system behavior by characterizing it in manual mode, and 2) to compare its performance with the automatic mode. Therefore, we carried out experiments similar to the

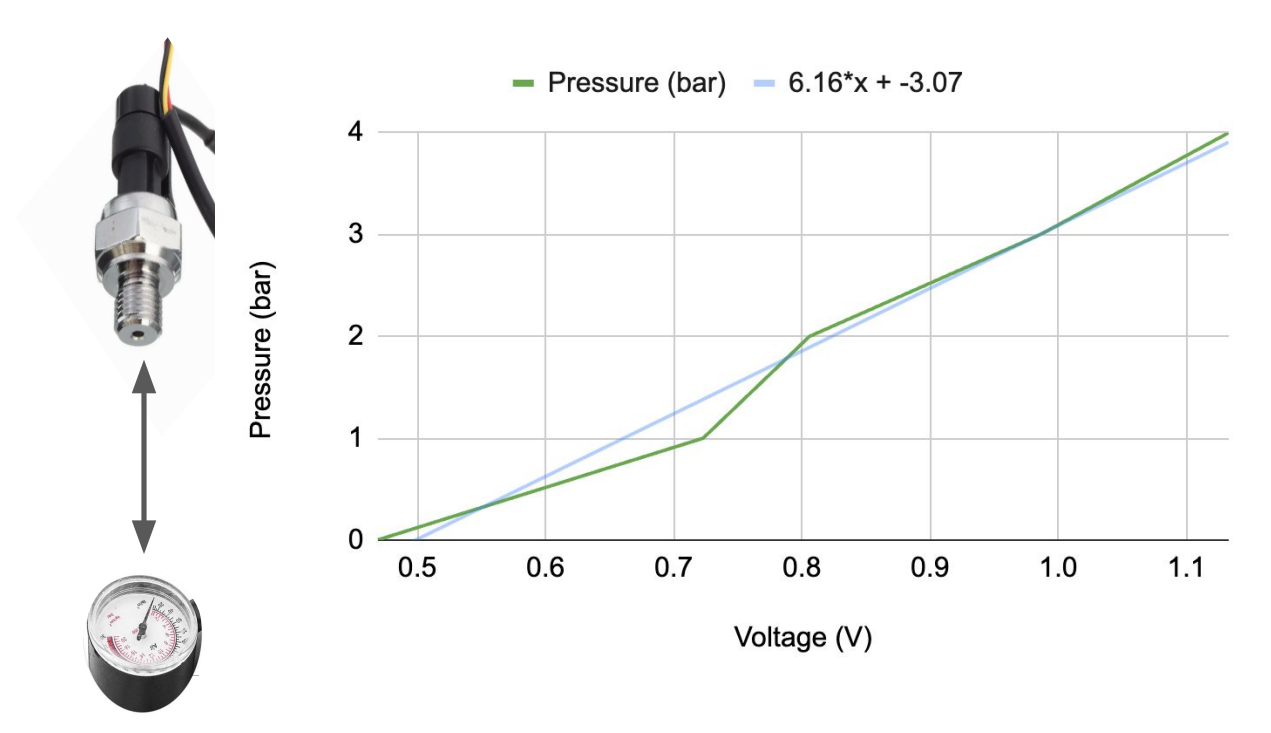


Figure 3: Sensor calibration against the pressure chamber gauge. The corresponding linear fit approximation of sensor voltage reading and applied pressure (variable 'x' corresponds to the measured voltage) can be observed (line in blue) and compared against experimentally observed values (in green).

conventional approach of SWP determination when done manually, and evaluated the proposed system in terms of successful measurement (or ability to see the dry-to-wet transition under pressurization) and time per measurements for both manual and automatic modes.

2.3. AI-Assisted Visual Detection of Stem Wetness

We implemented manual and automatic modes as shown in Fig. 5a. For the manual mode, the host computer itself (Raspberry Pi Model 3B) is connected to a monitor via HDMI and displays real-time video of the xylem, as no heavy computation is required and both video and control signals can be processed locally. For the automatic mode, to implement the AI-assisted visual object detection algorithm described below, and to enable real-time video and sensor data processing deemed critical for accurate pressure measurements and safety, a local stream of both video (in h264 format) and pressure sensor values was conducted from the host computer to a GPU-enabled client computer using a local network and assigned IP address. Both video stream and sensor data can be accessible to a client computer via an HTML webpage (an instance of the latter is shown in Fig. 5b), and therefore any device (even a mobile phone) can be able to access the data. To process video data, however, a laptop with an onboard GPU was utilized. A *commaseparated-value* (CSV) file was generated after every run and contained the timestamp and pressure readings from the sensor, so values can be correlated with the video to confirm data validity.

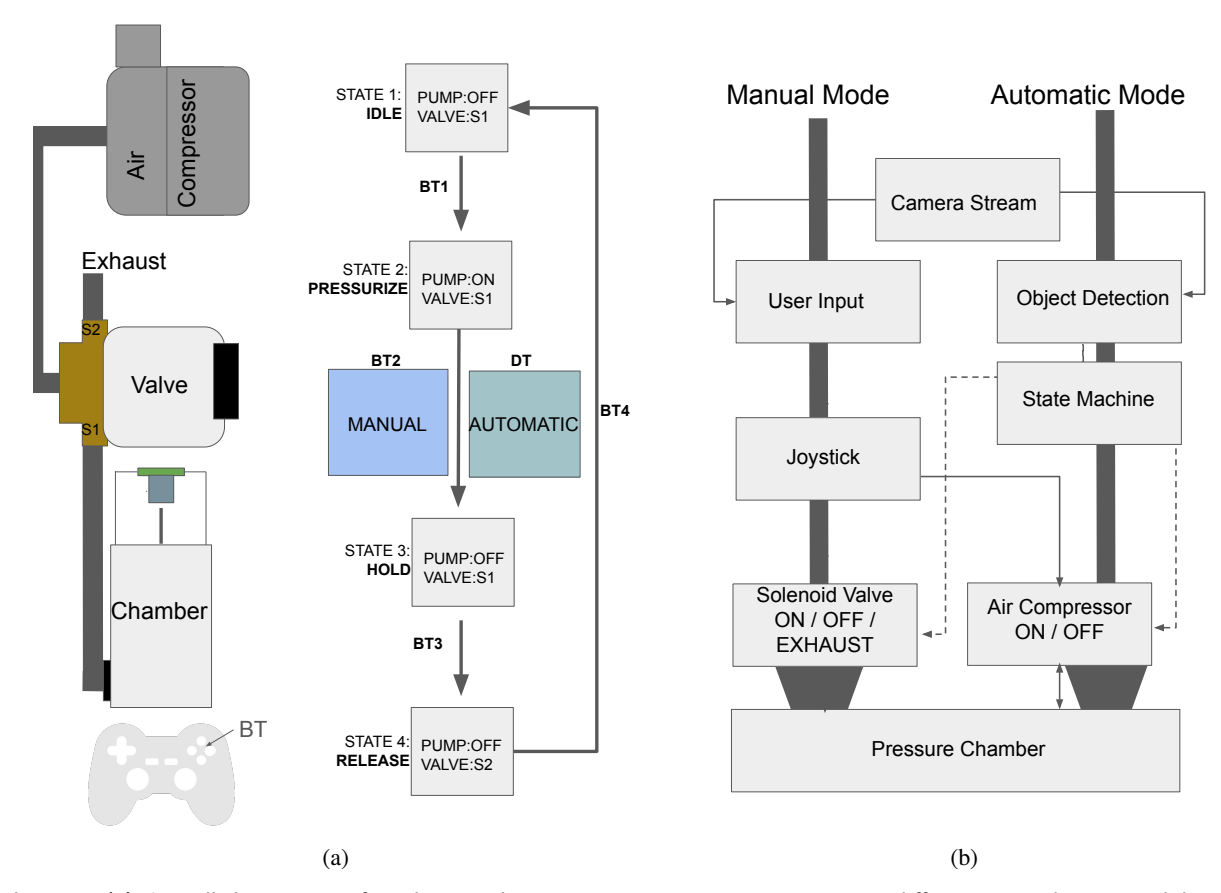


Figure 4: (a) Overall description of implemented states. Here BT1 to BT4 represent different joystick inputs while DT is the inference result from the object detection model trained on SWP determination data. (b) Modes of operation for our proposed system. A camera focused on the xylem streams video data to a local network in real time. In remote (manual) mode, the human operator can control both the air input to the chamber (via air compressor) as well as the direction of flow (via solenoid valve) based on real-time video observations utilizing a joystick. For autonomous operation, an object detection algorithm utilizing the video stream is combined with a state machine, and can automatically track xylem wetness.

In this work we employed an AI-assisted visual perception algorithm for object detection; i.e. to detect the xylem in the video feed and to determine its wetness status (dry/wet). The method chosen for our application was the *You Only Look Once* (YOLO) object detection and classification technique (Redmon et al., 2016). In earlier work (Dechemi et al., 2023), we evaluated the capacity of different versions of YOLO networks to detect the xylem and its wetness status. The YOLO network was trained from scratch on 7759 images using two sets of hyperparameters: baseline and tuned. The baseline used default settings, while the tuned version adjusted specific hyperparameters to evaluate the effects of various data augmentations on model performance and training duration. The adjustments included reduced saturation, added rotation, and removed mixup and paste-in augmentations, shifting the focus from color space to spatial-level transformations based on findings that color is not a stable feature in wetness detection. This approach aimed to make the models more sensitive to spatial features. Training was conducted on a Tesla P100 GPU for 80 epochs using an SGD

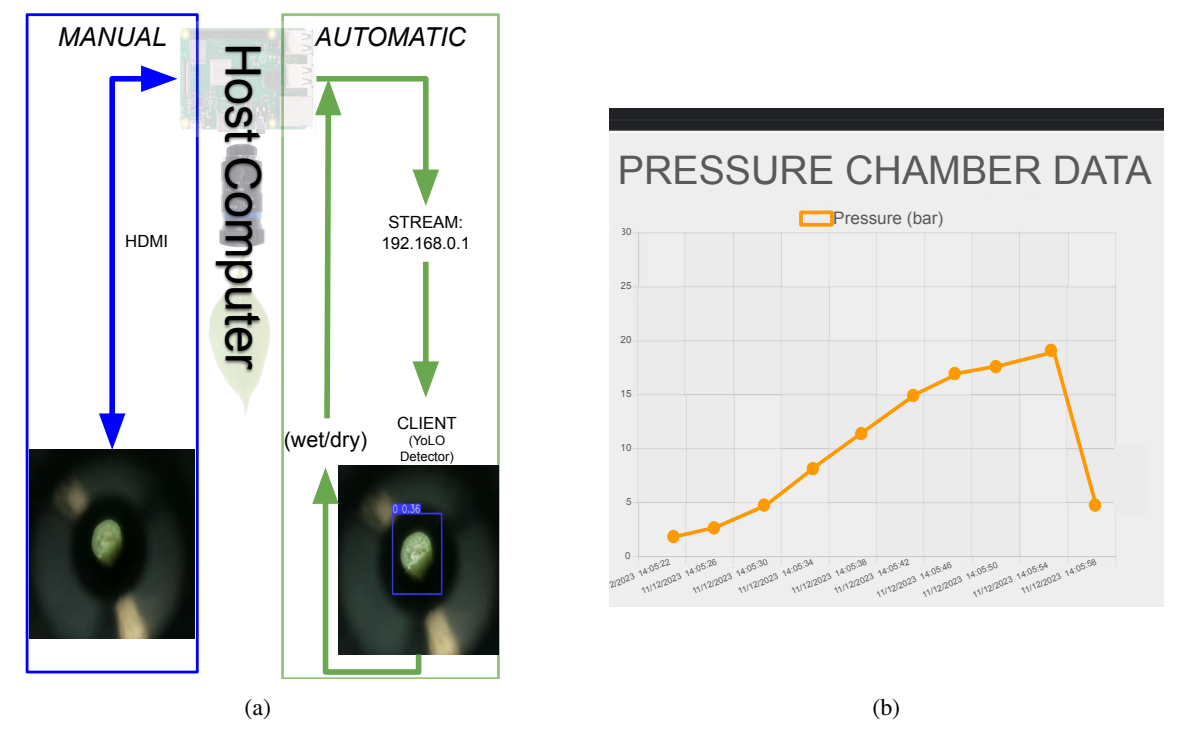


Figure 5: (a) Implementation of manual and automatic modes. In manual mode, the video output is directly connected to the host computer via HDMI, whereas in automatic mode a video stream over the network is sent, and assessed (the state of the xylem) via a YOLO object detector running on the client computer. The result of the latter is sent back to the host computer for controlling the solenoid valve. (b) Screenshot of the live-streamed data from the sensor to a webpage.

Table 1 Inference results for the YOLOv5 network (Dechemi et al., 2023).

161

162

163

164

165

166

167

168

169

	Execution time (s)	Average Inference Speed per Image/Frame (ms)	Classification Accuracy %	Stable Transition
Cloud-based (Tesla P100)	26.5	8.8	100	N/A
Edge-based (Jetson NX on test image)	449.4	448.4	100	N/A
Edge-based (Jetson NX on test video)	N/A	568.1	N/A	Yes

optimizer. As seen in Table 1, inference results from the tuned YOLOv5 model excelled in accuracy and confidence; thus, this model was adopted in our implementation in the current work.³

This inference result from the YOLO network (denoted as DT in Fig. 4) dictates the transition from the PRESSURIZE state (while DT = 0 or "dry" xylem) to the HOLD state (DT = 1 or "wet" xylem). Inference results from the network are sent from the client to the host computer for control signal processing; after detection and transition to the HOLD state, the system awaits user input to RELEASE the pressure and restart the cycle. Although implemented locally, it is worth mentioning that our system allows for internet connectivity with minor modifications, which would facilitate both offload computation to a cloud service instead or further permit remote access of the live stream cycle by human operators located anywhere in the world.

 $^{^{3}}$ For more details we refer the interested reader to Dechemi et al. (2023, Section IV).

70 3. Results

178

179

180

181

182

183

184

185

186

188

189

190

191

192

193

194

195

196

To verify our system's performance, experiments were conducted in an avocado tree field at the Agricultural Experimental Station (AES; 33° 58′ 3.2592″ N, 117°20′ 7.0296″W) at the University of California, Riverside. Avocado trees were selected because they constitute a highly salt- and drought-sensitive crop Gustafson (1976), and thus it is a high-value specialty crop that would directly benefit from more dense spatio-temporal SWP analysis afforded by our work. We collected data on two separate days: Day 1 (November 8^{th} , 2023, around 11 am) with dry weather and soil conditions, whereas Day 2 (November 15^{th} , 2023 around 10 am) was right after a rainy evening with high humidity in the air. We also performed both manual and automatic mode SWP determination. Details are listed next.

- On both days, a researcher utilized reflective foil bags to enclose various leaves from different trees, choosing a mix of shaded and unshaded regions (Fig. 6 left).
- After 10 minutes, leaves were excised from the trees, labeled, and put in an insulated bag (Fig. 6 center) for transportation to the laboratory facility where the system was set up, closely located (approximately 15 minutes) to the collection field.⁴
- The physical setup (Fig. 6 right) was used in the lab 15 minutes past excision to determine SWP under both manual (66%) and automatic (34%) modes during Day 1, and the manual mode alone during Day 2.
- After experiments, all video and pressure readings were verified using the generated CSV files, and plotted to compare the different modes proposed herein and reported SWP values.

3.1. Assessment of Manual Mode of Remote Operation

Considering the system validation in terms of different weather conditions (and its impact on SWP measurements), in-situ samples were collected over two different days. On the first day ("Day 1"), it had not rained for over a week, whereas on the second day ("Day 2"), sampling was done on a day after overnight rain. For both days, over 50 samples were collected and tested in manual mode, with results shown in Fig. 7 and Fig. 8.

In all experiments, the human operator was able to switch between the states described in Fig. 4 via joystick input, and the system promptly reacted in operating the air valve and compressor. Observed pressure values as well as resulting SWP measurements both lie within the expected range for the chosen crop and despite pressure sensor error of about 2%FS (0.4 bar), the manual mode can accurately represent a valid alternative to the conventional approach of the pressure chamber method. As expected, dryer weather contributed to more negative SWP values (average $\mu = -11.02$

⁴ While earlier literature was recommending making the measurements on the spot, it has been suggested that immediate storage of excised leaves in a cold and moist environment helps stabilize the sample's water potential and preserve the condition for hours or even days, depending on the species (Rodriguez-Dominguez et al., 2022).

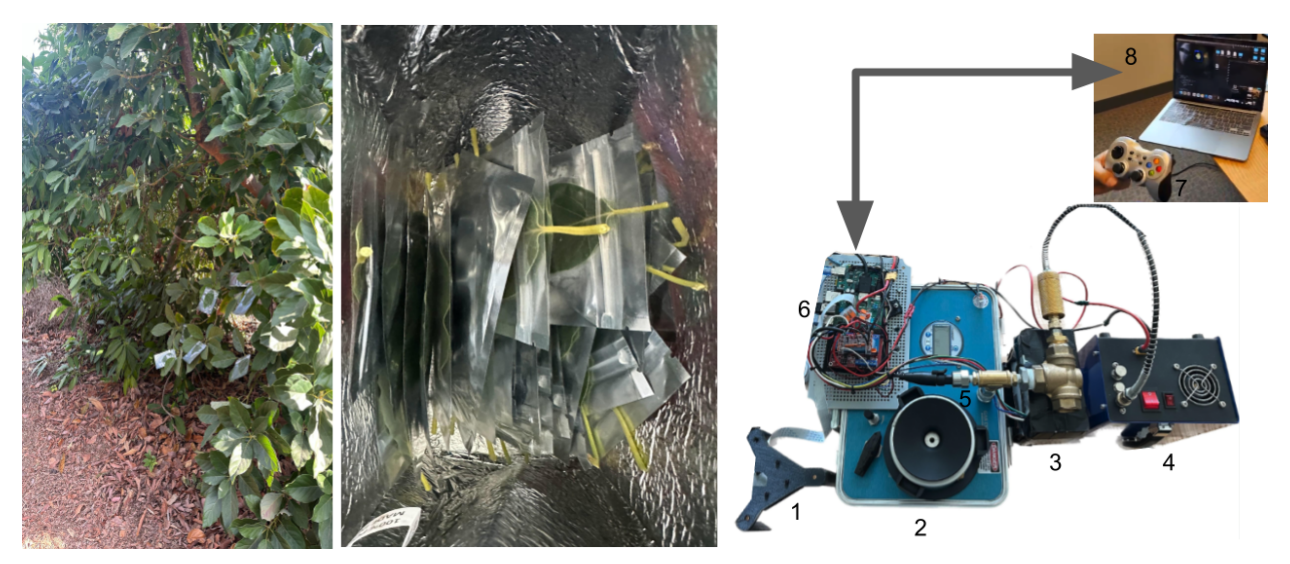


Figure 6: Data collection procedure. (Left) First, leaves were bagged close to noon local time and left to settle for 10 minutes. (Center) Leaves were then excised and transported in an insulated bag to the laboratory facility for prompt measurements. (Right) The physical testing setup: (1) camera and adapter, (2) pressure chamber, (3) electric solenoid valve, (4) air compressor, (5) pressure sensor, (6) Microcontroller boards and relays, (7) joystick, and (8) remotely connected laptop.

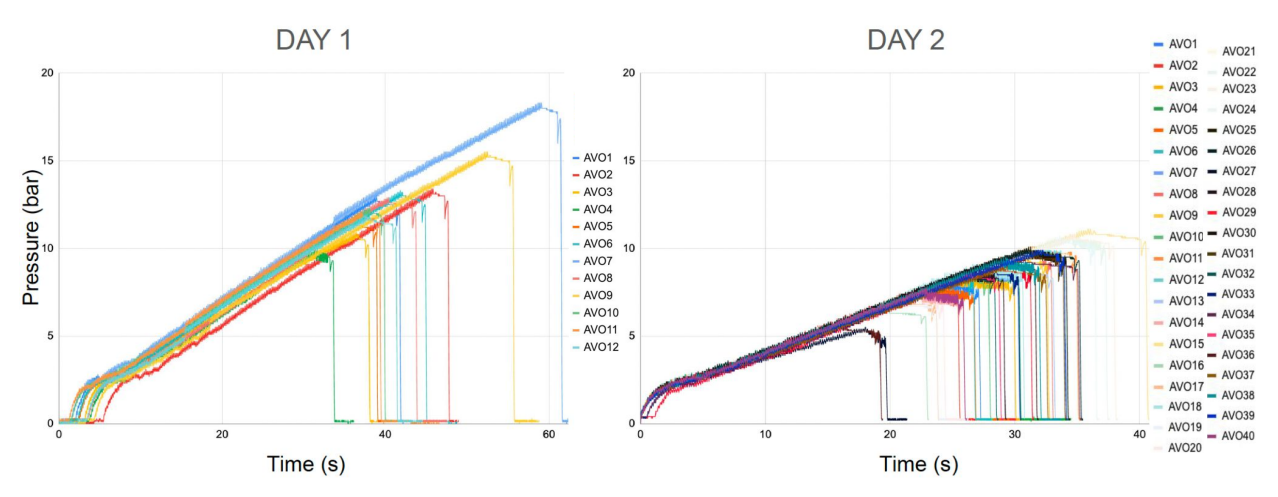


Figure 7: Graphical depiction of the attained experimental results in manual mode of operation for both days of in-situ data collection. (Left) On day 1, 12 samples were properly bagged and measured on a dry midday. (Right) On day 2, 40 samples were collected and tested midday after an overnight rain. In all cases, the pressure buildup inside the pressure increases smoothly, until the point that the user observes xylem water in the live video feed, and switches to hold, and the depressurize status. The differences between dry and wet environmental conditions in terminal pressure values and measurement times are visible.

bar, standard deviation $\sigma = 1.91$ bar) as compared to values obtained after rain (average $\mu = -5.11$ bar, standard deviation $\sigma = 1.17$ bar).

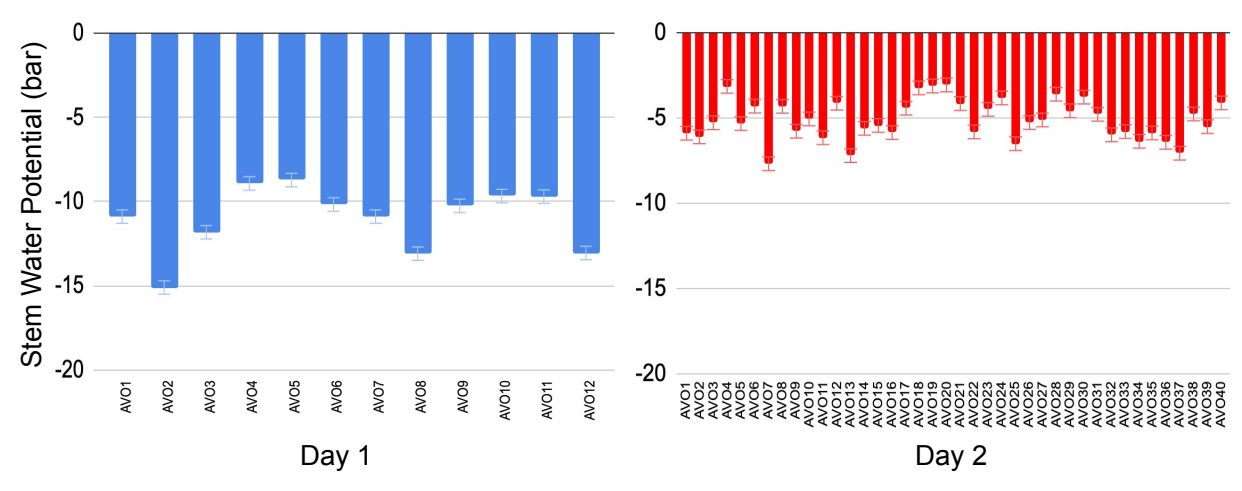


Figure 8: Determined SWP values from manual mode of operation experiments on both days. It can be seen that, as expected, smaller values were observed on Day 2 since measurements took place after an overnight rain. Vertical bars indicate a sensor full-scale error of 2%.

3.2. Assessment of Automatic Mode of Remote Operation

During the automatic mode, we evaluated the system under two conditions: a real-time online evaluation and an offline validation. The former condition aimed at testing samples collected on Day 1 according to the automatic implementation, while the latter considered an offline validation of the videos collected on Day 2 for assessing the detection itself. Since detection is the critical aspect of the automatic mode for the system to operate correctly, we wanted to verify how well the chosen AI-assisted visual objector detector would perform on recorded videos.

As seen in Fig. 9, real-time experiments were successfully conducted, resulting in an automatic reaction of the system (understood as turning off the pump) upon detection of water in the xylem. In Fig. 10 (left), detection of the "dry" state (A) would allow the operator to initialize the pump (shown as an arrow in the right panel), and automatically shut it off when detecting water in the xylem (B) from the live video stream. The final SWP calculated values are shown in Fig. 11 (average $\mu = -12.45$ bar, standard deviation $\sigma = 1.92$ bar), which are compatible with those reported for Day 1 in manual mode configuration.

For the offline evaluation, 40 video recordings of experiments were used to test the detector. In 35 out of 40 cases, the network was able to correctly classify the transition state of water appearance in the xylem. With reference to Fig. 12, the detector was robust under various lighting conditions and focus levels and was able to correctly classify the "wet" states with over 90% accuracy. Failed cases were caused either because of an erroneous detection (i.e. reporting "dry" instead of "wet" and vice versa) or no detection at all. Some sample failure cases are depicted in Fig. 13.

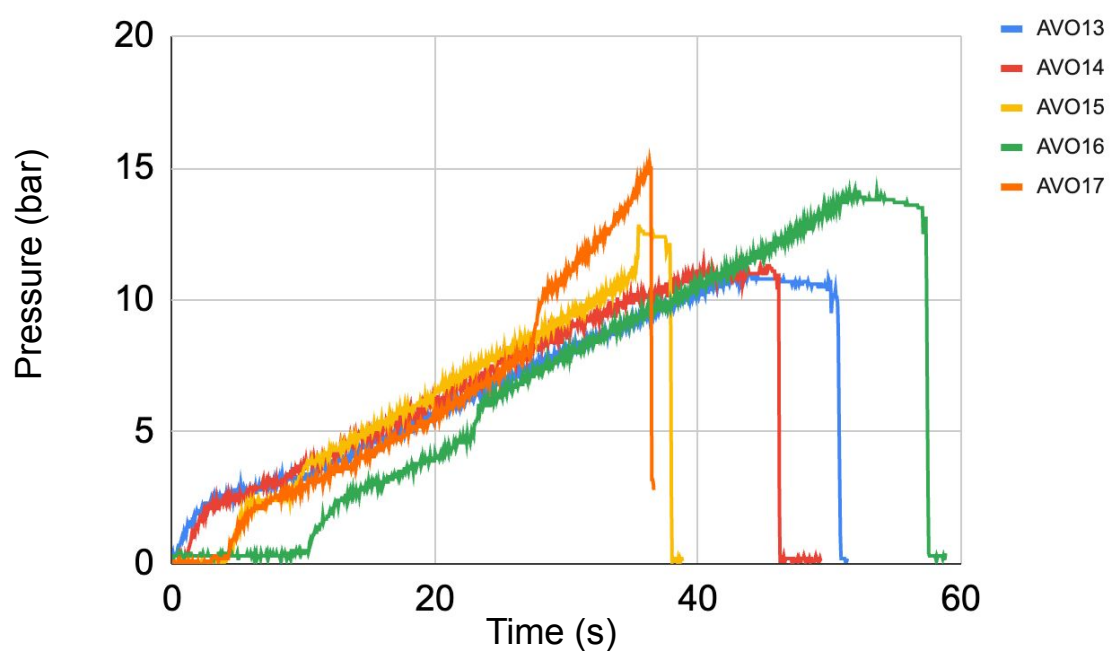


Figure 9: Graphical depiction of the attained results during the real-time evaluation of the automatic mode of operation on Day 1. The pressure builds up automatically, until the point that Al-assisted detection determines the status of the xylem has changed from dry to wet and then signals the hold and depressurize status, with no input from the human operator. The attained pressures and measurement times are consistent with those attained via the manual mode on Day 1 (left panel of Fig. 7).

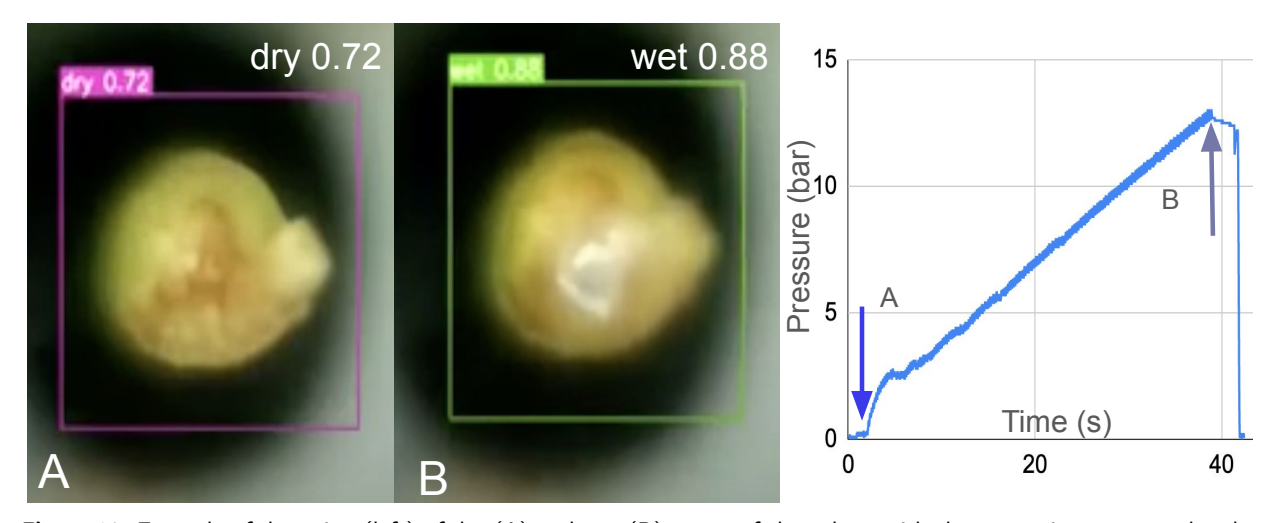


Figure 10: Example of detection (left) of dry (A) and wet (B) states of the xylem, with the respective pressure chamber sensor readings (right) during automatic mode operation.

3.3. Assessment of Operation Time in both Modes

We also calculated the average time per measurement cycle for both modes, considered here as the time between STATE 2 and STATE 3. Results are summarized in Table 2. It can be readily verified that both cases on Day 1 had a very similar cycle time. Although not conclusive, a slightly shorter time for the automatic method may anecdotally infer

217

218

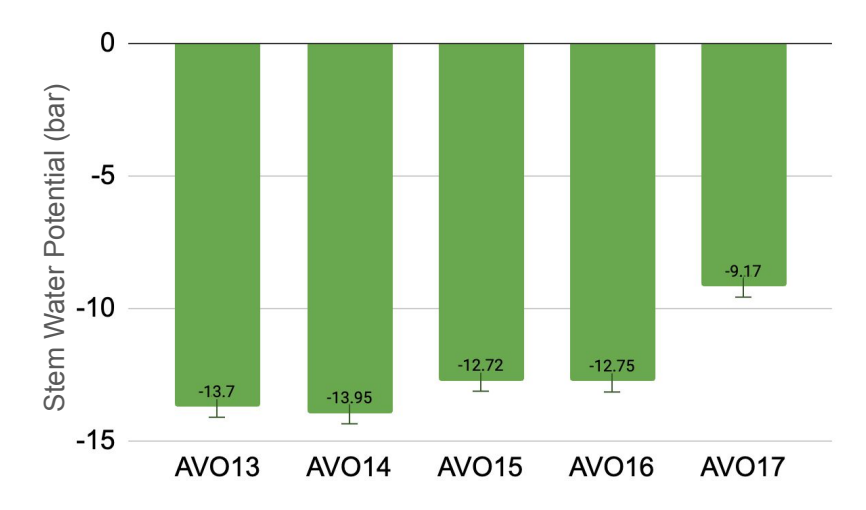


Figure 11: Automatically determined SWP values from the real-time automatic mode of operation experiments on Day 1. Values are consistent with those attained via the manual mode on Day 1 (Fig. 8).

Table 2
Average Time of Measurement per Sample.

	Average μ (s)	S.D. σ (s)
MANUAL (DAY1)	37.32	7.44
MANUAL (DAY2)	27.32	4.86
AUTO (DAY1)	35.65	4.9

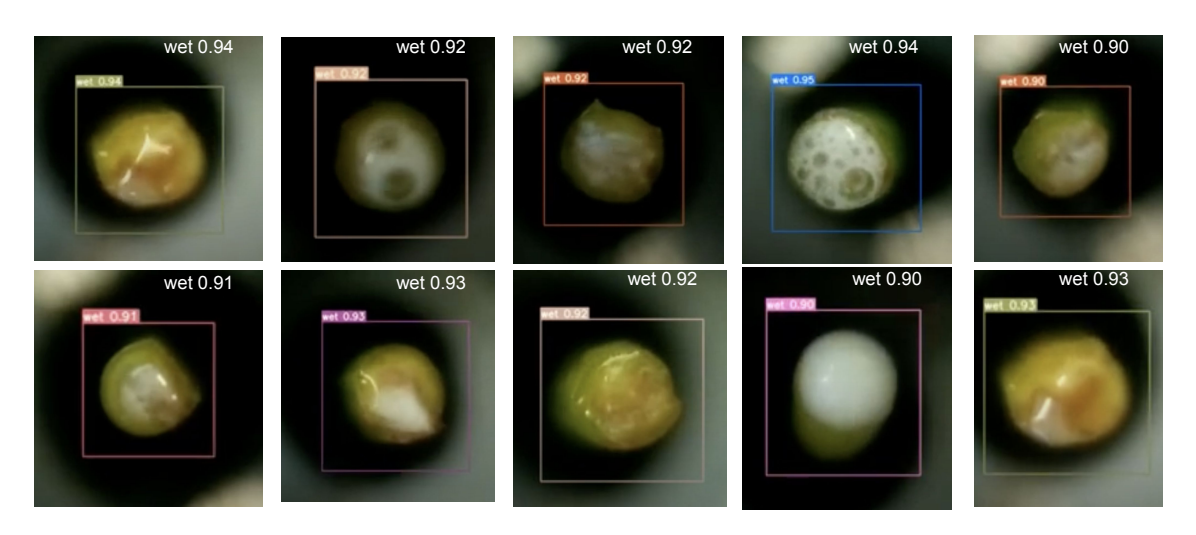


Figure 12: Sample detection results from offline evaluation.

a faster reaction time of the detector compared to a human when considering the point of measurement. In addition, since logs of pressure data and video recordings are provided by the system, the operator can confirm whether the chosen SWP value reflects the current determined result. The average cycle time for Day 2 in manual mode (27.32 s) was considerably less than the reported values of SWP for Day 1 (37.32 s) due to the overnight rain, which was also expected since the reported pressure values were lower.

220

221

222

223

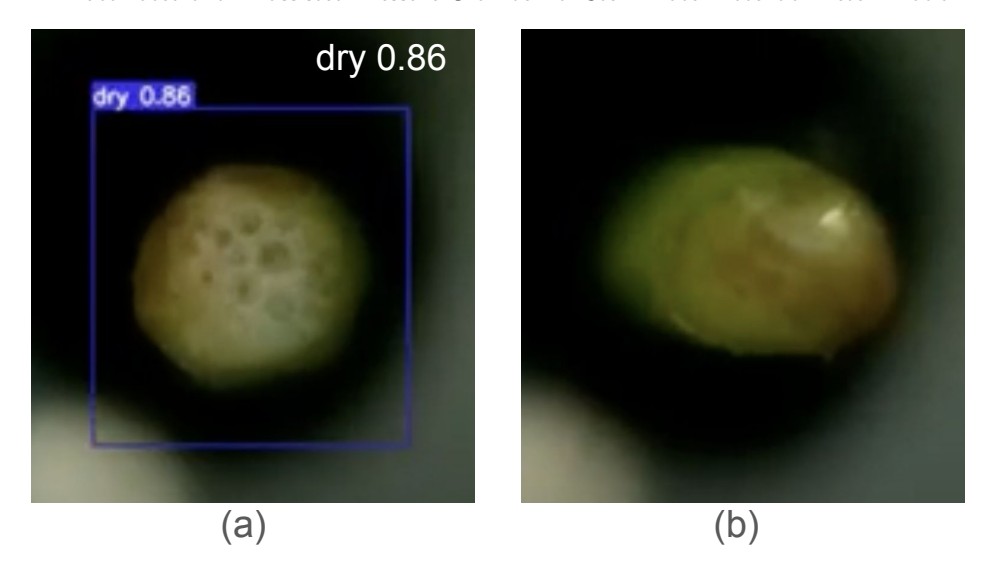


Figure 13: Examples of (a) incorrect and (b) no detection cases.

4. Discussion

Our goal was to make current pressure chamber systems more portable and safer and to improve the number of measurements that conventionally take place in situ, as opposed to a constrained number of measurements dependent upon the gas cylinder volume. To this end, one important modification included in our proposed system was the use of an air compressor instead of a pressurized gas cylinder. Our system, therefore, had to withstand the required pressure range and be able to report correct pressure readings while allowing repeatability and robustness.

By design, all components were selected to withstand the working pressure range. Further, our system was able to successfully perform numerous repeated measurements across all cases presented before as well as preliminary feasibility testing that took place before field deployment and assessment. In all cases, measurements were reported to the human operator in a direct and accessible manner, without any observed performance degradation. This translated to a high repeatability rate and data throughput, both of which are highly desirable in a tool for assessing water status.

Our system's capacity to perform actions comparable to a human operator in terms of the sequence of operations, detection, and improved cycle time, besides its affordability, indicate that it can serve as a viable alternative to measuring in-situ SWP when determining the water status of specialty crops, such as avocado trees. Finally, our method can even improve validation when utilizing other sensing modalities, such as proximal sensing by Microtensiometer (Pagay et al., 2014) or Hydrogel Nanoreporters (Jain et al., 2021).

Our main design consideration that led us to develop an "add-on" mechanism compatible with commercially available pressure chambers was made in order to minimize cost of acquisition for a user, considering that there is typically at least one "traditional" pressure chamber available to users that need to make SWP measurements. Indeed,

despite the additional upfront cost for the bill of materials to automate the pressure chamber as proposed, the operational cost over time makes our proposed solution more financially viable in the mid- and long-term. We hope that such a design consideration can help increase the chances for a higher adoption rate since no new pressure chamber other than those already in the field would need to be purchased or modified. Additionally, this design attempts to match in simplicity the interaction with the pressure chamber, since this is one of the main advantages of the method. However, if desired, our proposed system can be made as a standalone device by essentially adding a pressure-rated container with an input and output air connection, a pressure gauge, and the ability to securely fit a lid that can expose the stem's excised end to atmospheric pressure while keep the rest of the leaf inside the container.

The proposed system also allows for safer and more intuitive operation and SWP determination by removing the need for direct physical observation by looking through a magnifying glass. Even the seemingly modest integration of a camera and broadcasting the collected video feed in a screen can immediately make a difference. When coupled with automatic detection, then the amount of physical labor required to make multiple SWP measurements is expected to drop. In future work, we aim to test this hypothesis by performing user studies with agronomists and growers who rely on SWP assessments to optimize irrigation schedules for crops (Fulton et al., 2014).

During automatic detection, we considered the trained model from Dechemi et al. (2023), which aside from been fine-tuned with data from in-situ sampling, it was not retrained with any data collected in this study. Despite this, results were positive and attest to the suitability of AI-assisted visual perception of stem xylem wetness. In future work, we aim to collect additional data, including from other crops, and perform a larger analysis and evaluation of other AI-assisted object detection methods as well. These data will be curated and made available to the community to stimulate further research in the area.

5. Conclusion

This work introduced the first automated pressure chamber device capable of determining stem water potential (SWP) remotely and autonomously. The developed system was designed to be compatible with off-the-shelf pressure chamber devices for in-situ measurements, and it can allow for remote connection in real-time, while also logging relevant data and video recordings for post-measurement verification. To assess the utility of our proposed system, we performed in-situ data collection of several samples under different weather conditions and evaluated it in two operation modes: manual and automatic. The main difference in these is that in the former a user is looking at the video feed and determines when xylem water expression is observed, whereas in the latter an AI-assisted visual object detection algorithm is employed to determine xylem water expression. Results indicate that our automated chamber can perform correct measurements accurately, repeatably, and fast, while facilitating the role of the human operator in that no direct physical observation is required. This research paves the way for integrating the device with mobile

An Automated and Al-assisted Pressure Chamber for Stem Water Potential Determination

robots to achieve complete autonomous measurement of SWP, further minimizing the need for human intervention in this process.

Despite the successful demonstration of this prototype, our system has some limitations that can be improved in 277 the future. We have not considered an air-flow regulator added in series to our system. An electronic flow control 278 valve would be able to provide adjustable airflow and therefore improve the pressure profile precision and accuracy, 279 especially near the transition between states. Further, our experimental procedure was limited to avocado trees and 280 would benefit, especially in terms of automatic detection, by testing with additional crops. Finally, even though we 281 proposed an automatic mode for detecting water in the xylem, the system still requires human input to perform a full 282 cycle. While this was a deliberate choice made for safety, it would be useful to investigate a fully autonomous procedure 283 as well. 284

References

- Awad-Allah, E.F., 2020. Indispensable measuring techniques for water relations of plants and soils: A review. Open Journal of Soil Science 10, 616–630.
- Ball, R., Oosterhuis, D., 2005. Measurement of root and leaf osmotic potential using the vapor-pressure osmometer. Environmental and Experimental
 Botany 53, 77–84.
- Boyer, J.S., Knipling, E.B., 1965. Isopiestic technique for measuring leaf water potentials with a thermocouple psychrometer. Proceedings of the
 National Academy of Sciences of the United States of America 54, 1044.
- Campbell, M., Dechemi, A., Karydis, K., 2022. An integrated actuation-perception framework for robotic leaf retrieval: Detection, localization, and cutting, in: IEEE/RSJ International Conference on Intelligent Robots and Systems (IROS), pp. 9210–9216.
- Dechemi, A., Chatziparaschis, D., Chen, J., Campbell, M., Shamshirgaran, A., Mucchiani, C., Roy-Chowdhury, A., Carpin, S., Karydis, K., 2023.
- Robotic assessment of a crop's need for watering: Automating a time-consuming task to support sustainable agriculture. IEEE Robotics & Automation Magazine 30, 52–67.
- Dhillon, R.S., Upadhaya, S.K., Rojo, F., Roach, J., Coates, R.W., Delwiche, M.J., 2017. Development of a continuous leaf monitoring system to predict plant water status. Transactions of the ASABE 60, 1445–1455.
- Donovan, L., Linton, M., Richards, J., 2001. Predawn plant water potential does not necessarily equilibrate with soil water potential under well-watered conditions. Oecologia 129, 328–335.
- Elsayed, S., Mistele, B., Schmidhalter, U., 2011. Can changes in leaf water potential be assessed spectrally? Functional Plant Biology 38, 523–533.
- Fulton, A., Grant, J., Buchner, R., Connell, J., 2014. Using the pressure chamber for irrigation management in walnut, almond and prune. UC

 Cooperative Extension.
- Goldhamer, D., Fereres, E., et al., 2001. Simplified tree water status measurements can aid almond irrigation. California Agriculture 55, 32–37.
- Gonzalez-Dugo, V., Zarco-Tejada, P., Nicolás, E., Nortes, P.A., Alarcón, J., Intrigliolo, D.S., Fereres, E., 2013. Using high resolution uav thermal imagery to assess the variability in the water status of five fruit tree species within a commercial orchard. Precision Agriculture 14, 660–678.
- 307 Gustafson, D., 1976. Avocado water relations. JW Sauls, 47-53.
- Husken, D., Steudle, E., Zimmermann, U., 1978. Pressure probe technique for measuring water relations of cells in higher plants. Plant Physiology 61, 158–163.

An Automated and Al-assisted Pressure Chamber for Stem Water Potential Determination

- Jain, P., Liu, W., Zhu, S., Chang, C.Y.Y., Melkonian, J., Rockwell, F.E., Pauli, D., Sun, Y., Zipfel, W.R., Holbrook, N.M., et al., 2021. A minimally
- disruptive method for measuring water potential in planta using hydrogel nanoreporters. Proceedings of the National Academy of Sciences 118,
- e2008276118.
- Kan, X., Thayer, T.C., Carpin, S., Karydis, K., 2021. Task planning on stochastic aisle graphs for precision agriculture. IEEE Robotics and
- Automation Letters 6, 3287–3294.
- Levin, A.D., 2019. Re-evaluating pressure chamber methods of water status determination in field-grown grapevine (vitis spp.). Agricultural water
- management 221, 422–429.
- McCutchan, H., Shackel, K., 1992. Stem-water potential as a sensitive indicator of water stress in prune trees (prunus domestica l. cv. french).
- Journal of the American Society for Horticultural Science 117, 607–611.
- Mucchiani, C., Zaccaria, D., Karydis, K., 2024. Assessing the potential of integrating automation and artificial intelligence across sample-destructive
- methods to determine plant water status: A review and score-based evaluation. Computers and Electronics in Agriculture .
- Oosterhuis, D., Wullschleger, S., 1989. Psychrometric water potential analysis in leaf discs, in: Gases in plant and microbial cells. Springer, pp.
- 322 113_133
- Pagay, V., Santiago, M., Sessoms, D.A., Huber, E.J., Vincent, O., Pharkya, A., Corso, T.N., Lakso, A.N., Stroock, A.D., 2014. A microtensiometer
- capable of measuring water potentials below- 10 mpa. Lab on a Chip 14, 2806–2817.
- Redmon, J., Divvala, S., Girshick, R., Farhadi, A., 2016. You only look once: Unified, real-time object detection, in: IEEE Conference on Computer
- Vision and Pattern Recognition (CVPR), pp. 779–788.
- Rodriguez-Dominguez, C.M., Forner, A., Martorell, S., Choat, B., Lopez, R., Peters, J.M., Pfautsch, S., Mayr, S., Carins-Murphy, M.R., McAdam,
- S.A., et al., 2022. Leaf water potential measurements using the pressure chamber: Synthetic testing of assumptions towards best practices for
- precision and accuracy. Plant, Cell & Environment 45, 2037–2061.
- Rossello, N.B., Carpio, R.F., Gasparri, A., Garone, E., 2019. A novel observer-based architecture for water management in large-scale (hazelnut)
- orchards. IFAC-PapersOnLine 52, 62–69.
- 332 Schaible, G.D., Aillery, M.P., 2012. Water Conservation in Irrigated Agriculture: Trends and Challenges in the Face of Emerging Demands.
- Technical Report EIB-99. U.S. Department of Agriculture, Economic Research Service.
- 334 Scholander, P.F., Hammel, H.T., Hemmingsen, E.A., Bradstreet, E.D., 1964. Hydrostatic pressure and osmotic potential in leaves of mangroves and
- some other plants. Proceedings of the National Academy of Sciences of the United States of America 52, 119.
- Teng, H., Wang, Y., Song, X., Karydis, K., 2023. Multimodal dataset for localization, mapping and crop monitoring in citrus tree farms, in:
- 337 International Symposium on Visual Computing, Springer Nature Switzerland Cham. pp. 571–582.
- Vellidis, G., Liakos, V., Porter, W., Tucker, M., Liang, X., 2016. A dynamic variable rate irrigation control system, in: Proceedings of the International
- 339 Conference on Precision Agriculture, pp. 1–9.
- ³⁴⁰ Villagrán, S., Correa, C., Radrigán, R., 2011. A prototype of automatic pressure pump (type schölander pump). Acta Horticulturae, 609–616.